nature communications

Article

https://doi.org/10.1038/s41467-025-58083-z

Mimicry of molecular glues using dual covalent chimeras

Received: 27 May 2024

Accepted: 7 March 2025

Published online: 24 March 2025

Check for updates

Eden Kapcan[1,2,3], Karolina Krygier[1,2,3], Maya da Luz[2], Nickolas J. Serniuck[1,2,3], Ali Zhang[4], Jonathan Bramson[1,4] & Anthony F. Rullo[1,2,3,4]

A special class of proximity inducing bifunctional molecules/chimeras called molecular glues leverage positive co-operativity to stabilize ternary complex formation and induce a biological response. Despite their utility, molecular glues remain challenging to rationally design. This is particularly true in the context of inducing cell-cell proximity which involve ternary complexes that comprise non- or negatively interacting proteins. In this work, we develop a dual proximity labeling strategy enabling a chimera to covalently crosslink a non-interacting serum antibody to a tumor surface protein, within a ternary complex. The resultant resistance to dissociation, including in the presence of competitor binding ligands, mimics molecular glue stabilization. We demonstrate these covalent glue mimics (CGMs) can induce cell-cell proximity in three distinct model systems of tumor-immune recognition, leading to significant functional enhancements. Collectively, this work underscores the utility of dual proximal covalent labeling as a potential general strategy to stabilize ternary complexes comprising non-interacting proteins and enforce cell-cell interactions.

Proximity-inducing chimeras represent a growing class of novel bifunctional therapeutic modalities, with special utility across a diverse range of disease indications[1,2]. These bifunctional molecules (BMs) generally increase the effective molarity between two proteins in a ternary complex to enact a biological response. A special class of BMs called molecular glues leverage positive co-operativity to drive and stabilize ternary complex formation, enhancing this response[3,4]. Here, molecular glue binding to both proteins is more thermodynamically favorable than binding to either protein alone, which drives ternary complex formation in the forward direction (illustrated in Fig. 1, K_{ter} vs. K_{bi}). As a result, the ternary complex is now stable to dissociation and the presence of free competitor binding ligands. A key example is the anti-cancer drug Rapamycin, which templates inhibitory ternary complexes between FKBP and the kinase mTOR, the latter a key regulator of tumor growth and proliferation. Here, Rapamycin binding to FKBP first, dramatically increases Rapamycin apparent affinity for mTOR (and vice versa) due to stabilizing protein-protein interactions[3].

"Glue-like" stabilization of ternary complexes is especially strategic when endogenous species concentrations are low relative to their K_d for binding the BM, and/or when competitive protein binding ligands are present. The discovery and development of BMs with glue-like properties is challenging however, especially for applications that aim to bridge non-interacting proteins or proteins that interact unfavorably within the ternary complex, the latter associated with negative co-operativity[5,6]. These scenarios are likely to be encountered when bridging receptors on the surfaces of two cells to induce "cell-cell proximity". Fundamental efforts in tumor immunotherapy leverage bi-specific biologic or small molecule chimeric modalities to induce cell-cell proximity. One key example uses antibody recruiting BMs to enhance immune cell recognition and elimination of tumor cells[7–10]. Here, the BM must form stable ternary complexes comprising a tumor antigen (e.g., urokinase-type plasminogen activator receptor (uPAR)) and serum antibody. Immune cell Fc receptors subsequently engage these ternary complexes, leading to tumor eradication. One key challenge to induced cell-cell proximity

[1]Center for Discovery in Cancer Research, McMaster University, Hamilton, ON, Canada. [2]Department of Chemistry and Chemical Biology, McMaster University, Hamilton, ON, Canada. [3]Department of Medicine, McMaster University, Hamilton, ON, Canada. [4]Department of Biochemistry and Biomedical Sciences, McMaster University, Hamilton, ON, Canada. e-mail: rulloa@mcmaster.ca

https://doi.org/10.1038/s41467-025-58083-z

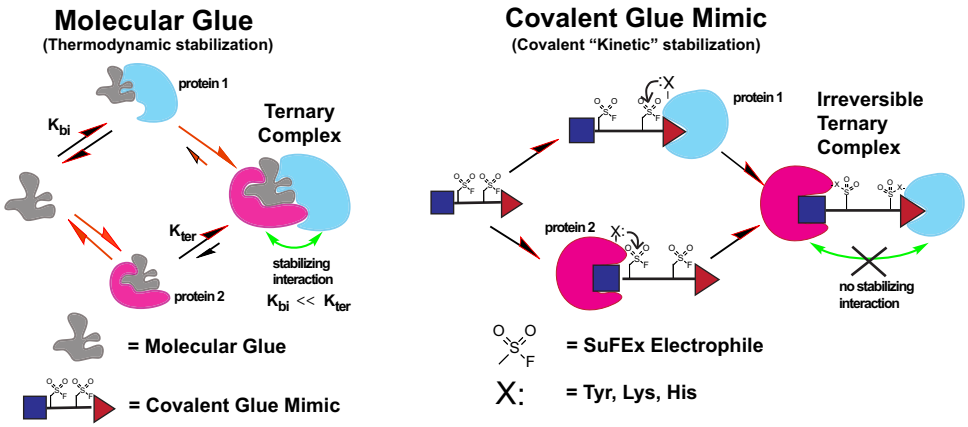

Fig. 1 | Schematic depiction of molecular glues versus covalent glue mimics. Molecular glues (MGs) use positive cooperativity to stabilize a ternary complex thermodynamically. Covalent Glue Mimics (CGMs) use strategically positioned dual covalent labeling sulfur(VI) fluoride exchange (SuFEx) electrophiles to form kinetically irreversible ternary complexes. K_{bi} = equilibrium constant for binary complex formation, K_{ter} = equilibrium constant for ternary complex formation.

surrounds the stability of bridging ternary complexes in the presence of opposing biological forces. In addition to steric clashing between tumor and immune cells, immune activation via Fc receptor clustering/synapse formation proceeds through mechanical re-arrangement events. Collectively, these forces can destabilize even thermodynamically favorable protein/ternary complexes as observed in the case of "slip bonds"[11,12]. Thus, the ability to even partially stabilize cell-cell proximity in a "glue-like" manner is highly strategic.

The lack of available molecular glues to stabilize complexes comprising non-interacting proteins and induce cell-cell proximity inspired our efforts to devise a strategy that "kinetically" mimics molecular glue stabilization using covalency. We envisioned that this could be accomplished using bifunctional chimeric molecules that irreversibly crosslink both protein binding partners of the ternary complex, preventing dissociation. This requires the BM to both selectively discriminate *between* the two ternary complex proteins, and also preferentially crosslink these proteins versus abundant off-target proteins. We hypothesized this could be achieved by functionalizing the BM at two optimal positions with pre-organized electrophiles, each activated upon binding to its cognate ternary complex binding partner. Importantly, this strategy leverages pre-organized electrophile-kinetic effective molarity enhancements to enforce selective crosslinking with proximal binding site residues, thus providing access to diverse endogenous proteins lacking cysteine. For this reason, we chose aryl sulfonyl fluorides, a Sulfur(VI)-Fluoride Exchange (SuFEx) electrophile, for incorporation into hetero-bifunctional molecules (Fig. 1)[9,10,13,14]. SuFEx electrophiles react with diverse amino acids proximal to the binding site, are hydrolytically stable, and can be efficiently incorporated into complex chimeric molecular formats containing peptides or carbohydrates[9,10,14–16].

Recently in fact, an elegant dual covalent crosslinking "glue discovery" approach was reported, that uses two *reversible* electrophiles to crosslink a molecular glue fragment with two *interacting* proteins. Here the authors use two chemoselective aldehyde and disulfide electrophiles to selectively crosslink cysteine on ERRγ with a lysine on 14-3-3[17].

In the current work, we report the development of covalent glue mimics (CGMs) that selectively irreversibly covalently cross-link two different *non-interacting* endogenous proteins, enforcing ternary complex formation. Uniquely, CGMs template these ternary complexes despite intrinsic destabilization from likely negative binding cooperativity. In both macrophage and NK cell-based models of cell-cell induced proximity, we demonstrate that CGM covalent crosslinking of antibody with the uPAR tumor antigen enables significant functional enhancements compared to covalent engagement of either antibody or tumor antigen alone. Stable engagement of CGMs with the tumor cell surface is also observed to strategically prevent competition from urokinase, an ultra-high affinity endogenous competitor ligand for uPAR, whose binding drives cancer metastasis. Additionally, we show that CGMs can induce direct T cell-tumor proximity and affect tumoricidal function using T cells engineered with universal receptors specific for CGM. More broadly, this work demonstrates that the optimal pre-organization of two SuFEx electrophiles on a single chimera can affect efficient selective irreversible crosslinking of two *non-interacting* endogenous proteins with therapeutic function. Importantly, high covalent crosslinking selectivity can be achieved between endogenous proteins lacking chemoselective cysteine residues. Altogether, we disclose dual covalent proximity inducing molecules capable of driving biomolecular interactions that lack positive co-operativity.

Results

Evaluation of bifunctional molecules that covalently engage *either* ternary complex protein

Mono-covalent bifunctional molecules (cBM) were chemically synthesized to covalently engage either anti-dinitrophenyl (DNP) IgG antibody or urokinase plasminogen activating receptor (uPAR) in a ternary complex (Supplementary Fig. S3, S4). uPAR represents a well-established target widely expressed in a variety of cancer types. uPAR is also involved in several tumor growth processes, including metastasis via binding to its endogenous high affinity ligand, the urokinase plasminogen activator (uPA)[18]. Anti-DNP represents an established model serum antibody that activates immune cells when recruited to tumor cells, however, it possesses no intrinsic ability to bind uPAR. Non-covalent control molecules (BM) were also synthesized to discern covalent versus non-covalently stabilized ternary complexes (Supplementary Fig. S1, S2). To engage uPAR, BMs/cBMs were equipped with a uPAR binding peptide derived from the literature "AE133" peptide[19]. This was appended to a DNP ligand to engage anti-DNP IgG through an optimized linker, which we established was critical to mediate ternary complex formation (Supplementary Fig. S12). To enable the covalent engagement of uPAR or anti-DNP, a single aryl sulfonyl fluoride "SuFEx" electrophile was incorporated site-specifically into BM peptide scaffolds via solid phase peptide synthesis to generate cBMs (Supplementary Fig. S11).

We began by evaluating two cBMs, ^{uPAR}cBM and ^{Ab}cBM, each containing a single SuFEx insertion, in a Bio-Layer Interferometry (BLI) ternary complex binding assay (Fig. 2). ^{Ab}cBM places the SuFEx close to the DNP binding ligand while ^{uPAR}cBM places the SuFEx directly on the C terminus of the uPAR binding peptide. The initial locations chosen for electrophile installation aim to strike an optimal balance between tightly pre-organizing the SuFEx to react with the target

https://doi.org/10.1038/s41467-025-58083-z

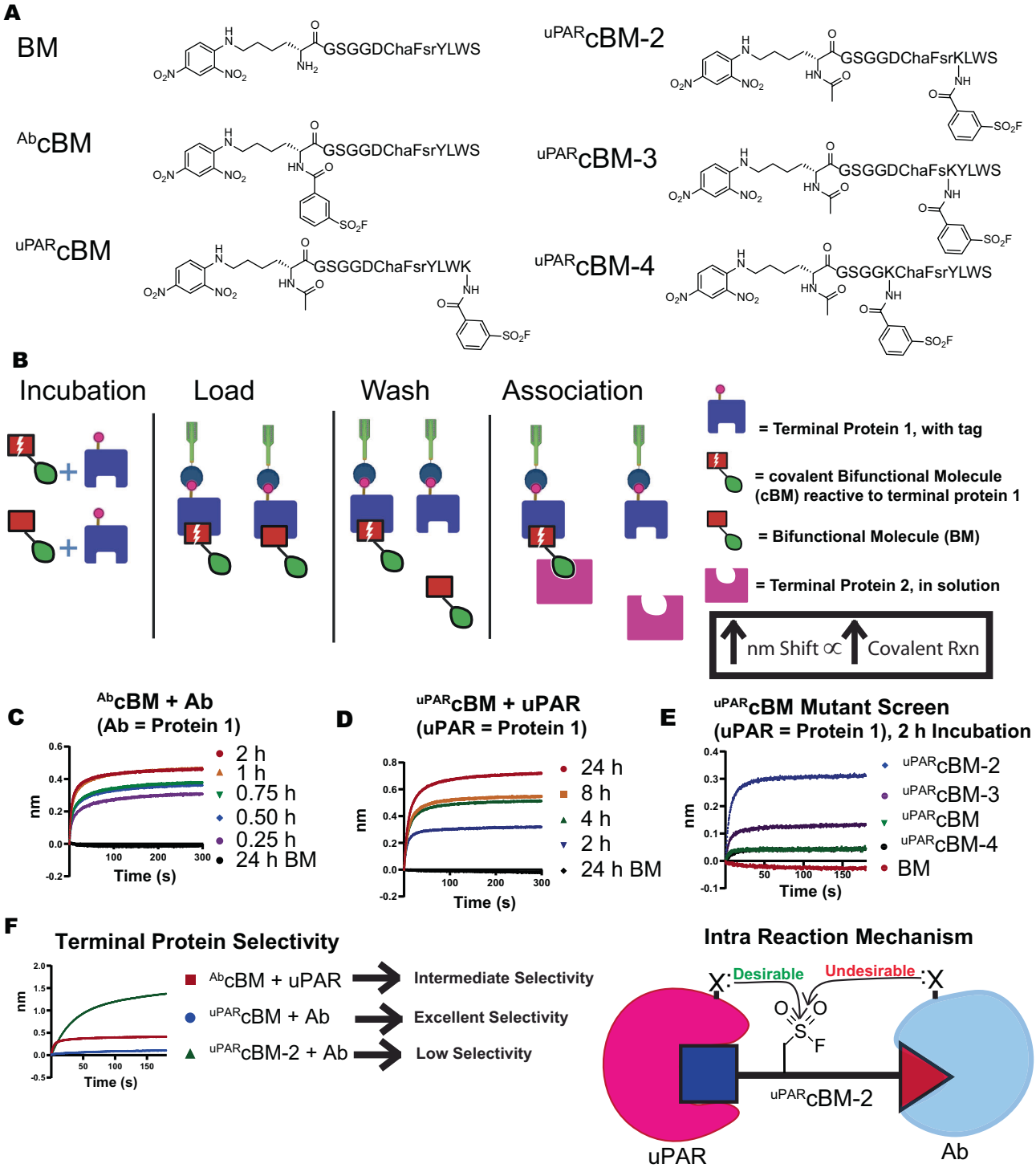

protein of interest upon binding, and maximizing the distance between this SuFEx group and the second ternary complex protein after binding. The goal was to identify cBMs that can selectively label only uPAR (^{uPAR}cBM) or only anti-DNP Ab (^{Ab}cBM) versus off-target proteins. This would identify the two optimal positions to insert two SuFEx electrophiles on the bifunctional molecule, furnishing the desired covalent glue mimic (CGM) that crosslinks uPAR with anti-DNP in a ternary complex.

BLI assays begin with an initial incubation step where the compound is incubated with one of the ternary complex proteins (i.e. Protein 1 = uPAR or Anti-DNP Ab) containing an affinity tag (Fig. 2B). This complex is then loaded onto a biosensor through the affinity tag, followed by a series of wash steps to remove non-covalent complex. In the final step, the soluble terminal protein is added (Protein 2), which leads to the formation of the ternary complex and a concomitant association signal. Therefore, only ternary complexes stabilized by a covalent linkage generate an association signal. Incubations with either ^{uPAR}cBM or ^{Ab}cBM led to an increase in association signal as a function of increasing incubation times with Protein 1 (i.e., antibody or uPAR) (Fig. 2C/2D). In control experiments, baseline association signal was observed when anti-DNP was substituted with non-specific isotype IgG, or, uPAR substituted with bovine serum albumin (BSA), supporting covalent reaction selectivity (Supplementary Fig. S13). Baseline association signal was observed when non-covalent BM was used (which

Fig. 2 | Validation of cBMs in biosensor assays. A BM and cBM chemical structures. Covalent Bifunctional Molecule "^{Ab}cBM" is designed to selectivity react with Anti-DNP. Covalent Bifunctional Molecule "^{uPAR}cBM", is designed to selectivity react with uPAR. The design of analogs ^{uPAR}cBM (2-4) were informed by uPAR:AE133 analog co-crystal structures to enhance uPAR labeling kinetics **B** Schematic of BLI assays. Incubation: cBM is incubated with biotinylated terminal protein 1. Load: the incubation solution is loaded onto a streptavidin biosensor for 3 minutes. Wash: Probes are submerged in buffer wells to remove non-covalent complex for 3 minutes. Association: Probes are submerged in a solution containing soluble terminal protein 2, giving rise to association signal proportional to covalent reaction for 5 minutes. Created in BioRender. Kapcan, E. (2025) https://BioRender.com/k18a082 (**C**) 300 nM ^{Ab}cBM incubation with 75 nM anti-DNP for different periods of time indicated (terminal protein 1 = anti-DNP, terminal protein 2 = 500 nM uPAR). D. 300 nM uPAR-cBM incubation with 75 nM uPAR for different periods of time indicated (terminal protein 1 = uPAR, terminal protein 2 = 250 nM anti-DNP). The association plateau achieved following each incubation reaction time was divided by the final association plateau reached at reaction completion to calculate the fraction covalent reaction at each incubation time. This data was used to generate the reaction kinetic plots shown in Supplementary Fig. S14. Experiments described in Figs. 2C and 2D were completed in duplicate with biologically independent samples. **E** A repeat of the experiment in (**D**) using next generation ^{uPAR}cBM derivatives. **F** Intra ternary complex selectivity assay. Here the same general format of the previous assays is followed, only protein 1 and 2 are swapped for each compound during the 24 h incubation step. i.e. ^{Ab}cBM (terminal protein 1 = uPAR, terminal protein 2 = anti-DNP), ^{uPAR}cBM (terminal protein 1 = anti-DNP, terminal protein 2 = uPAR). Zero association signal thus indicates complete intra ternary complex selectivity. A cartoon description of the undesired competitive labeling reaction between ^{uPAR}CBM−2 and anti-DNP versus the intended uPAR protein is included for clarity.

lacks a SuFEx electrophile), confirming non-covalent complex is dissociated during BLI wash steps. Collectively, these results support the ability of ^{uPAR}cBM and ^{Ab}cBM to form selective covalent complexes with uPAR or anti-DNP, respectively. For labeling studies using ^{Ab}cBM, we observed a fast increase in association plateau with time, which enabled estimation of anti-DNP antibody labeling kinetics (k_{obs} ~ 1.1 x 10^{-3} s^{-1}, Supplementary Fig. S14). For labeling studies using ^{uPAR}cBM, we observe a slower increase in association plateau with time, corresponding to a smaller rate constant (k_{obs} ~1.4 x 10^{-4} s^{-1}) for labeling uPAR (Supplementary Fig. S14). MALDI TOF/TOF analysis further confirmed the formation of covalent binary complexes ^{uPAR}cBM-uPAR and ^{Ab}cBM-anti-DNP (Supplementary Fig. S15). BLI assays were also conducted to define cBM binding affinities for anti-DNP and uPAR proteins, supporting a lower binding affinity for the latter (Supplementary Fig. S16, S17). Finally, fluorescent SDS-PAGE assays were also conducted as an orthogonal assay to evaluate cBM reaction kinetics (Supplementary Fig. S18), supporting the labeling rate and selectivity data obtained via BLI in Fig. 2.

Optimizing the reaction effective molarity of both electrophiles on a single bifunctional molecule is key to enforcing formation of the desired covalently cross-linked ternary complex versus labeling of two off-target proteins. Optimizing the reaction effective molarity is also critical to enable electrophile discrimination of/between the two bound ternary complex proteins. Importantly, this also disfavors two electrophiles reacting with the same bound protein. Since the antibody labeling rate was rapid, we set out to further increase the uPAR labeling rate. ^{uPAR}cBM was designed to minimize competitive antibody labeling at the expense of a slower uPAR labeling rate. Data from a literature uPAR/AE133 derivative co-crystal structure, however, suggested that installation of the electrophile closer to the AE133 *N* terminus, at the internal tyrosine position, would increase pre-organization with a potential SuFEx reactive tyrosine on uPAR (i.e. Y57), increasing labeling kinetics[20]. The results from a literature reported AE133 alanine scan suggested that this internal AE133 tyrosine and 2 additional residues (d-Arg, Asp), could be substituted with a SuFEx functionalized amino acid without perturbing uPAR binding. Therefore, we synthesized additional analogs ^{uPAR}cBM(2-4), with SuFEx substituted at one of these three locations, for evaluation in the BLI assays described above (Fig. 2E). In these assays, we observed that SuFEx positioning dramatically modulates the rate of uPAR labeling. ^{uPAR}cBM-2, predicted to maximize the proximity of SuFEx to Y57 on uPAR demonstrated the most rapid uPAR labeling.

Next, we sought to evaluate our design strategy for the capacity to covalently discriminate each protein *within* a ternary complex. A lack of proper discrimination or "intra selectivity" can occur because the binding of one protein (i.e. Protein 1) pre-organizes both electrophiles to react before binding to Protein 2. This represents a unique and significant challenge compared to conventional covalent inhibitor development which labels a single protein, most commonly through a chemoselective cysteine. To test this, we repeated the assays described above, however the cBM was incubated with the *opposite terminal* protein (i.e. ^{uPAR}cBM was incubated with anti-DNP Ab and ^{Ab}cBM was incubated with uPAR) before loading on biosensor probes (Fig. 2F). Although the opposite terminal protein still binds the respective cBM selectively, it is now positioned further from the reactive electrophile, a design element intended to decrease the reaction rate. In this assay, undesirable proximity labeling of the distal bound ternary complex protein will also lead to increases in the association signal. Here, we observed that uPAR incubations with ^{Ab}cBM for 24 h gave rise to lower association signal amplitudes below 0.4 nm, consistent with lower uPAR labeling from within the non-covalent binary complex compared to ^{uPAR}cBM. ^{uPAR}cBM ability to label uPAR gives rise to signal amplitudes > 0.6 nm under comparable conditions (Fig. 2D) with a half-life on the order of 1–2 h. ^{Ab}cBMs ability to rapidly label anti-DNP on the order of minutes, however, supports the ability of the electrophile at this position to discriminate between, and favor, reaction with bound antibody versus uPAR within a ternary complex. ^{Ab}cBM binding to the deep cleft on uPAR, positions the electrophile closer to the uPAR surface, explaining the observed low degree of uPAR labeling. Antibody incubations with ^{uPAR}cBM gave rise to baseline association signal amplitude, indicating a lack of labeling from within the non-covalent binary complex. This supports the ability of the SuFEx electrophile at this position on ^{uPAR}cBM to discriminate between and favor reaction with bound uPAR versus anti-DNP within a ternary complex. Antibody incubations with ^{uPAR}cBM-2, however, indicated efficient anti-DNP labeling from within the non-covalent binary complex. This can be rationalized by the closer positioning of the SuFEx to the DNP ligand compared to ^{uPAR}cBM. Despite the faster uPAR labeling kinetics potentially achievable, a covalent glue mimic (CGM) based on ^{uPAR}cBM-2 could also label anti-DNP via the electrophile intended for uPAR and fail to covalently crosslink the ternary complex. For this reason, we designed CGM to incorporate the two SuFEX electrophiles at the combined positions used in both ^{uPAR}cBM and ^{Ab}cBM.

Ternary complex covalent crosslinking using a Covalent Glue Mimic (CGM)

Lead CGM was synthesized (see methods section, Supplementary Fig. S2) and tested using a modified BLI Assay (Fig. 3A). In this assay, both biotinylated uPAR, and unmodified anti-DNP, are incubated together with one of CGM, ^{uPAR}cBM, ^{Ab}cBM, or BM, before loading onto the biosensor. Following the loading step, the probe is submerged in dissociation "wash" solutions containing uPAR competitor ligand followed by anti-DNP competitor ligand to remove non-covalent binding complexes (Fig. 3B). Successful ternary complex formation gives rise to an association signal during the loading step, but only covalently crosslinked ternary complexes are stable to dissociation in the presence of both uPAR and DNP competitor ligands. cBMs that link to uPAR (^{uPAR}cBMs) but not antibody will form ternary

https://doi.org/10.1038/s41467-025-58083-z

complexes that are dissociated by the presence of competitor anti-DNP binding ligand. Conversely, cBMs that link to antibody (^{Ab}cBMs) but not uPAR, will form ternary complexes that are dissociated by the presence of competitor uPAR binding peptide ligand. In this experiment, we observed that each covalent compound gave rise to similar association plateaus, and that these plateaus were significantly higher than that achieved by non-covalent BM (Fig. 3C). Given the calculated affinities of BM for uPAR and anti-DNP (Supplementary

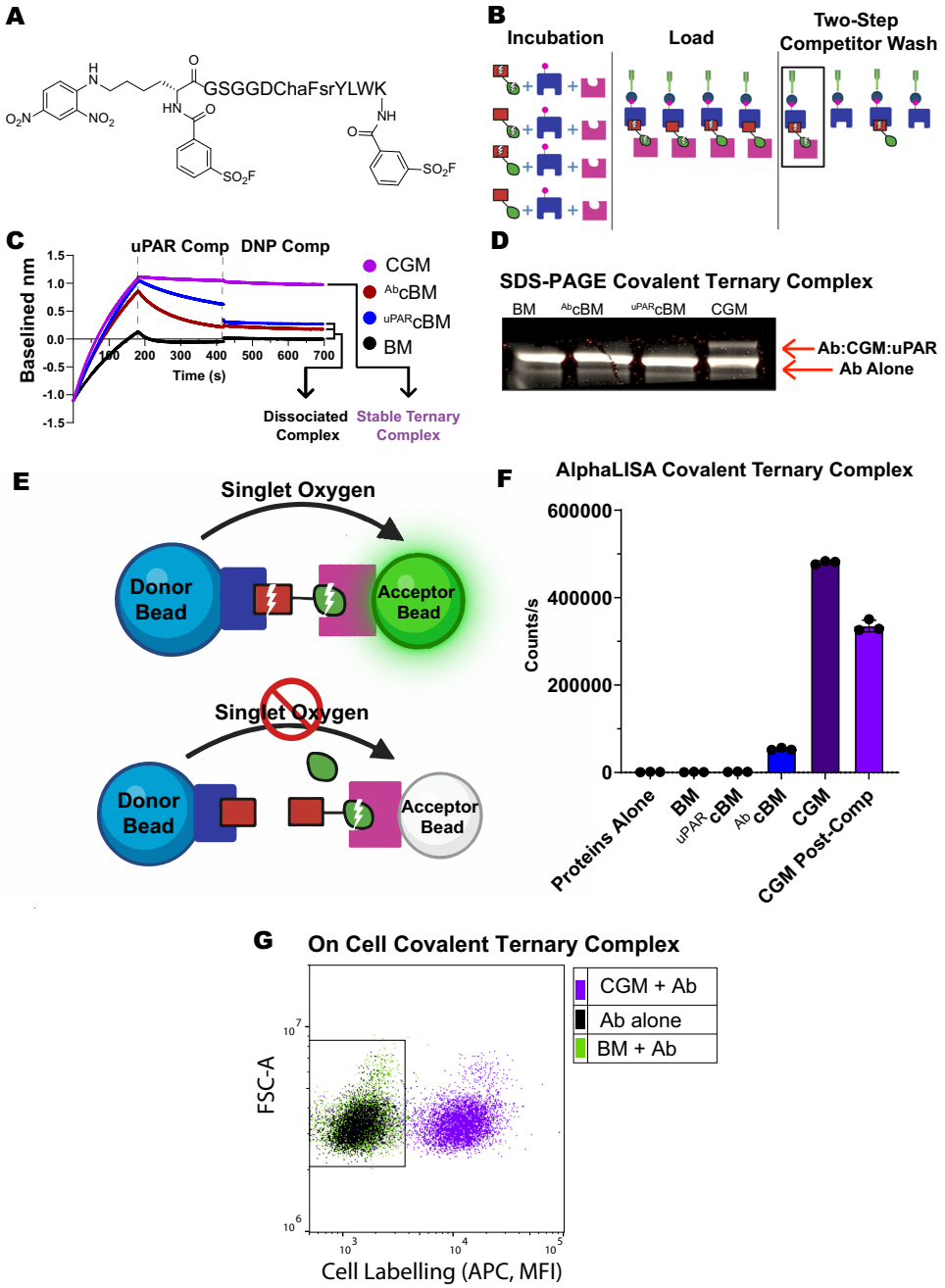

Fig. 3 | CGM templates covalently crosslinked ternary complexes. A Chemical structure of CGM. **B** BLI assay designed to evaluate covalent crosslinking within ternary complexes. In this format, 100 nM CGM is incubated with 100 nM biotinylated uPAR and 50 nM anti-DNP, for 24 hours. Next, this solution is loaded onto a streptavidin biosensor probe for 3 minutes. Next, the probe is submerged in a solution of 10 μM free uPAR competitor, for 4 minutes (first wash step). Finally, the probe is placed in a solution of 50 μM free DNP competitor, for 5 minutes (second wash step). Created in BioRender. Kapcan, E. (2025) https://BioRender.com/x85u298 (**C**) BLI sensorgram from covalent ternary complex assays evaluating CGM versus ^{uPAR}cBM, ^{Ab}cBM or BM. **D** Orthogonal SDS-PAGE assay to probe covalently crosslinked ternary complex formation, using Coomassie protein staining. 0.6 μM Anti-DNP Ab is incubated with 2.5 μM Chimera and 2 μM uPAR overnight, then loaded onto a gel, stained for 1 hour, and destained overnight. The experiment was conducted twice with results in close agreement. **E** Schematic depiction of the AlphaLISA assay. A solution of uPAR-biotin (300 nM), CGM (300 nM), and Anti-DNP (300 nM) is incubated overnight. The next day, uPAR and Anti-DNP competitors (10 μM, 50 μM respectively) are added in the post-competitor conditions (15 min). Next, they are incubated with Donor Streptavidin and Acceptor Anti-Fc beads (20 μg/mL) for 1 hour. Upon excitation of donor beads, singlet oxygen is released, and if in proximity to acceptor beads, a chemiluminescent reaction occurs, which correlates with ternary complex formed. Created in BioRender. Kapcan, E. (2025) https://BioRender.com/m58g121 (**F**) AlphaLISA assay to assess bead-bead ternary complex formation. Data was presented as mean +/− s.d. of $n = 3$ biologically independent samples. **G** Scatter plot generated from a flow cytometry antibody recruiting assay. uPAR+ A172 cells were incubated with 1 μM CGM or BM and 500 nM Anti-DNP Ab-AF647 for 4 hours at 37 °C, followed by wash steps. 10,000 events were collected. Gates were placed on the antibody alone (anti-DNP) condition.

Figs. S16, S17) this strongly supports the presence of destabilizing forces on the ternary complex and negative binding co-operativity. The comparable association signals between covalent compounds support their ability to form comparable amounts of ternary complexes, and with increased stability compared to BM. For ternary complexes mediated by ^{Ab}cBM, association signal quickly decreased during the first wash step, which contains free uPAR competitor ligand. This is consistent with the rapid dissociation of ^{Ab}cBM-Ab complexes from immobilized uPAR, supporting the ability of ^{Ab}cBM to covalently link to anti-DNP (which is free in solution) and reversibly bind uPAR (which is immobilized). This data also confirms the ability of ^{Ab}cBM to discriminate between uPAR and anti-DNP in a ternary complex. Ternary complex signal associated with the ^{uPAR}cBM condition decreased more slowly during the first wash step compared to ^{Ab}cBM, and rapidly during the second wash step, which contains the antibody binding competitor (free DNP). This observation is consistent with ^{uPAR}cBM covalently linked to uPAR on the probe and reversibly bound to anti-DNP. The slow dissociation observed during the first wash step containing uPAR competitor is attributed to the slow dissociation of anti-DNP antibody promoted by dilution effects. Dissociation of anti-DNP occurs with a half-life consistent with that calculated for anti-DNP binding to ^{uPAR}cBM-uPAR calculated in Supplementary Fig. S17. Outcompeting the uPAR interaction would have led to rapid dissociation, which does not occur due to the ^{uPAR}cBM-uPAR covalent linkage. In the second wash step, which contains DNP competitor, the remaining non-covalently bound anti-DNP rapidly dissociates from ^{uPAR}cBM linked to uPAR-coated probe. This result also supports the ability of ^{uPAR}cBM to covalently discriminate between uPAR and anti-DNP in a ternary complex and only label uPAR. Ternary complex signal associated with the CGM condition, however, remained unchanged in the presence of both DNP and uPAR competitor wash steps. This is consistent with complete conversion to covalently cross-linked ternary complex (Fig. 3C). Additional selectivity controls were tested via BLI supporting covalent ternary complex formation is dependent on selectivity for anti-DNP Ab (Supplementary Fig. S19).

As an orthogonal method to confirm the formation of covalently crosslinked ternary complex, we monitored the reaction by SDS-PAGE. The incubation of uPAR, anti-DNP and CGM led to the formation of a new larger molecular weight band corresponding to both ternary complex proteins, that is not observed using monocovalent analogs (Fig. 3D). Quantification of increased band intensity with incubation time by densitometry, enabled estimation of covalent crosslinking kinetics (Fig. S21) and a final product conversion to approximately 25% crosslinked ternary complex by 8 h. These kinetics appear to be similar to and likely limited by the uPAR labeling step, as anticipated. As observed for the respective binary cBM analogs, covalent ternary complex crosslinking was also observed to be highly selective (Supplementary Figs. S18, S20).

SDS-PAGE assays measure in-solution covalent ternary complex formation using soluble proteins. Next, we wanted to probe CGM ability to template these complexes between two surfaces to model cell-cell ternary complexes. This introduces additional destabilizing effects that accompany steric clashes between two proximal non-interacting and potentially repulsive surfaces like cells. To address this, we applied an AlphaLISA assay to model covalent ternary complex bridging of tumor and immune cell surfaces, where uPAR and anti-DNP IgG are immobilized to luminescent donor and acceptor beads (Fig. 3E). This assay is also designed to model the additional avidity enhancements to ternary complex formation, that accompany multivalent interactions between several ternary complexes, tumor antigens, and immune receptors on cells. Here, we observed significantly greater luminescence signal proportional to the number of donor and acceptor beads in close proximity in the presence of CGM versus monocovalent bifunctional cBM molecules (Fig. 3F, Supplementary Fig. S30, 31). Interestingly, the lack of signal observed for nM affinity binding BM and cBMs supports the destabilization of ternary complexes from negative co-operativity binding. In the presence of a cocktail of anti-DNP and uPAR competitors, signal associated with CGM samples retained approximately 70% signal. This observation supports the majority of bead-bead complexes formed are stabilized by selective covalent crosslinking. Overall, these results demonstrate the ability of CGMs to template more ternary complexes between model tumor and immune surfaces compared to cBM and BM, consistent with glue mimicry by the CGM. This is because ternary complexes are now stable to dissociation despite potential negative co-operative binding and the presence of abundant competitor ligands. Next, we evaluated CGM ability to covalently crosslink ternary complexes directly on the surface of tumor cells. Here, anti-DNP-AF647 conjugates were incubated with both CGM and uPAR+ A172 cells. The cells were washed to remove non-covalent complex, and their fluorescence measured by flow cytometry. We observed BM conditions gave rise to baseline cell-associated fluorescence, supporting the absence of ternary complexes. The CGM condition, however, led to a significant fluorescence increase that was resistant to wash steps, supporting covalently crosslinked ternary complex formation on the tumor cell surface (Fig. 3G). Collectively, this data supports the ability of a rationally designed dual electrophilic bifunctional chimera to stabilize cell surface ternary complexes comprising non-interacting proteins. Importantly, this strategy uniquely does not require the two endogenous proteins of interest to contain chemoselective cysteine amino acids.

CGM covalent engagement with tumor cell surface uPAR inhibits binding from endogenous competitor ligand urokinase

Proximity-inducing therapeutic applications are susceptible to inhibition by endogenous competitor ligands, especially in the absence of ternary complex positive co-operativity. Ternary complex formation with uPAR is similarly prone to inhibition from urokinase (uPA), a natural high affinity (*sub* nM) ligand for uPAR, whose binding initiates tumor proliferation and metastasis. Since CGMs were demonstrated to efficiently covalently engage cell surface uPAR, we anticipated they could template protein complexes resistant to uPA competition. Pending future in vivo validation studies, this could be useful if CGM can localize to uPAR prior to uPA trafficking and binding. To test this, we developed a microscopy assay to image the ability of CGM or BM to block uPA-AF647 conjugate binding to uPAR+ A172 cells (Fig. 4). In this assay, A172 cells are preincubated with CGM or BM for 1 h, followed by co-incubation with uPA-AF647 for 15 min. Using a fluorescence widefield microscope, we observed a substantial decrease in cell surface localized fluorescence in the presence of CGM compared to BM. This is consistent with increased blockade of the uPA binding interaction due to covalent stabilization of uPAR complexes with CGM. This data also supports the selective formation of covalently stabilized ternary complexes on the tumor surface via the uPA binding site on uPAR.

CGM induces cell-cell proximity and elicits greater efficacy compared to mono-covalent analogs in functional tumor immunotherapy assays

We sought to test the functional relevance of covalently crosslinked ternary complexes on immune function, using an established flow cytometry antibody-dependent cellular phagocytosis (ADCP) assay. This assay models macrophage tumoricidal function, which depends on the formation of antibody mediated ternary complexes on tumor cells. In this assay format, biotinylated uPAR, chimeras, and anti-DNP Ab are incubated overnight. The next day, this solution is added to fluorescent streptavidin microspheres to model cancer targets, and fluorescent U937 cultured macrophage immune cells. Cell-cell induced proximity through the formation of tumor antigen-immune complexes leads to target phagocytosis, which can be measured using 2-color flow cytometry. Here, we compared the ability of CGM to promote tumor

https://doi.org/10.1038/s41467-025-58083-z

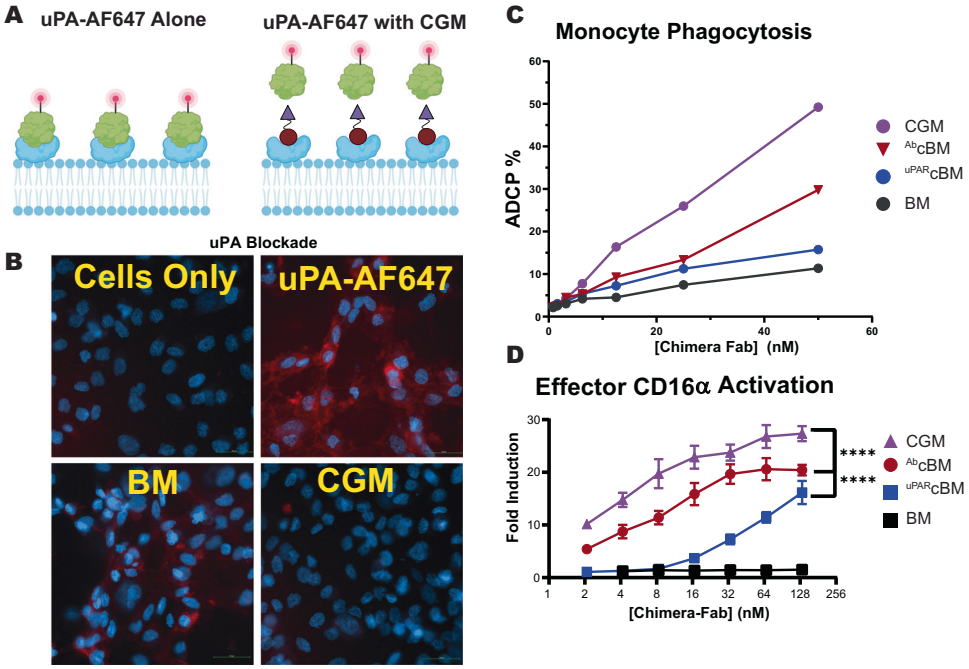

Fig. 4 | CGM elicits greater anti-tumor blockade and immunotherapeutic function compared to monocovalent bifunctionals. A Schematic depiction of the microscopy uPA-uPAR competition assay. uPA-AF647 alone leads to an increase in immunofluorescence. Incubation with CGM or BM leads to decreases in immunofluorescence. Created in BioRender. Kapcan, E (2025) https://BioRender.com/b47b948 (**B**) Immunofluorescence microscopy images depicting CGM versus BM mediated uPA blockade. Top Left: Cells only. Top Right: Cells + 25 nM uPA-AF647 for 15 minutes. Bottom Left: Addition of 100 nM BM to cells for 1 hour, followed by 25 nM uPA-AF647 for 15 minutes. Bottom Right: Addition of 100 nM CGM to cells for 1 hour, followed by 25 nM uPA-AF647 for 15 minutes. The green scale bar is equal to 50 microns. **C** Antibody dependent cell-mediated phagocytosis (ADCP) assay. 100 nM uPAR-Biotin, 200 nM chimera, and 100 nM anti-DNP Ab are incubated overnight. The next day this solution is added to fluorescent streptavidin microspheres to model cancer targets + fluorescent U937 cultured macrophage immune cells for 1 hour. Two-color flow cytometry is used to measure phagocytosis as described previously[22]. Data was presented as mean of $n = 2$ biologically independent samples. **D** CD16α activation antibody dependent cellular cytotoxicity (ADCC) assay[21]. Here, CD16+ Jurkat T cell lines are incubated with uPAR+ A172 cells, chimera, and anti-DNP antibodies. After 24 hours, luciferase-substrate is added to each well, and luminescence is measured, correlating to immune activation. Data was presented as mean +/− s.d. of $n = 3$ biologically independent samples. **** corresponds to p value < 0.0001 by Two-way ANOVA with Tukey's multiple comparison test.

target phagocytosis compared to ^{Ab}cGM, ^{uPAR}cGM, and BM. All compounds were able to selectively mediate ADCP, however, we observed a significant potency and efficacy advantage using the CGM, (Fig. 4C, Supplementary Fig. S22). These compounds were then evaluated in an FDA-approved monoclonal antibody CD16α activation assay which models natural killer cell anti-tumor function via antibody dependent cell mediated cytotoxicity (ADCC)[21]. Here, CD16+ Jurkat T cell lines are incubated with uPAR+ A172 cells, chimeras and anti-DNP Ab. Jurkat T cells are engineered to couple antibody-dependent CD16α activation to luciferase expression, resulting in a detectable "fold induction" signal increase. CGM was observed to selectively induce CD16 immune activation with a significant enhancement in both potency and efficacy compared to the other analogs (Fig. 4D, Supplementary Fig. S23). Interestingly, no dose of BM or monocovalent analogs could match the efficacy achieved via CGM, despite the likelihood that the number of ternary complexes formed are comparable. This supports previous reports on the importance of kinetically stabilizing tumor-immune receptor complexes to enforce receptor activation signaling[12,22–24].

Covalent stabilization of tumor antigen binding within cell-cell ternary complexes induces T cell-tumor cell proximity, leading to tumor eradication

In addition to antibody-based proximity-inducing strategies, universal T cell approaches have emerged as a promising cellular tumor immunotherapeutic strategy. Here, the T cell is engineered with a receptor that recognizes a chimera, which in turn templates a ternary complex with tumor antigens to activate tumoricidal function[25]. Using a recently described universal T cell system engineered with a synthetic antigen receptor (SAR) that recognizes the DNP ligand, we evaluated CGM's ability to activate universal T cell tumoricidal function[24]. Using live cell imaging, we measured T cell cytotoxic function in response to compound treatment in a co-culture system comprising DNP-specific SAR-T cells and GFP+ uPAR-expressing A172 glioma cells (Fig. 5). We observed 100% tumor cell cytotoxicity using only 1 nM of CGM or ^{uPAR}cBM in contrast to ^{Ab}cBM and BM. Additional experiments demonstrate CGM and ^{uPAR}cBM have some cytotoxic activity at 250 pM, which is lost by 62.5 pM (Supplementary Fig. S24). The same trend was observed in T cell proliferation assays where T cell proliferation in response to SAR engagement serves as a measure of T cell activation via cell-cell induced proximity (Supplementary Fig. S25). Additional controls demonstrate uPAR is necessary for SAR T cell activation (Supplementary Fig. S26). Despite high affinity binding via BM and comparable ternary complex formation, covalency appears critical for cell-cell induced proximity, leading to tumoricidal function. Interestingly, this observation suggests in the context of direct immune T cell engagement, covalency to the tumor antigen alone within the ternary complex may be sufficient to achieve optimal tumoricidal immune function.

Optimizing conversion of covalent crosslinking of ternary complexes

The sub quantitative conversion of covalently crosslinked ternary complexes observed in gel assays may represent an underestimate of what happens in the context of proteins immobilized on surfaces (e.g. BLI, AlphaLISA, cells). If this estimation is truly reflective of crosslinking conversion, it demonstrates even sub-stoichiometric conversion of

https://doi.org/10.1038/s41467-025-58083-z

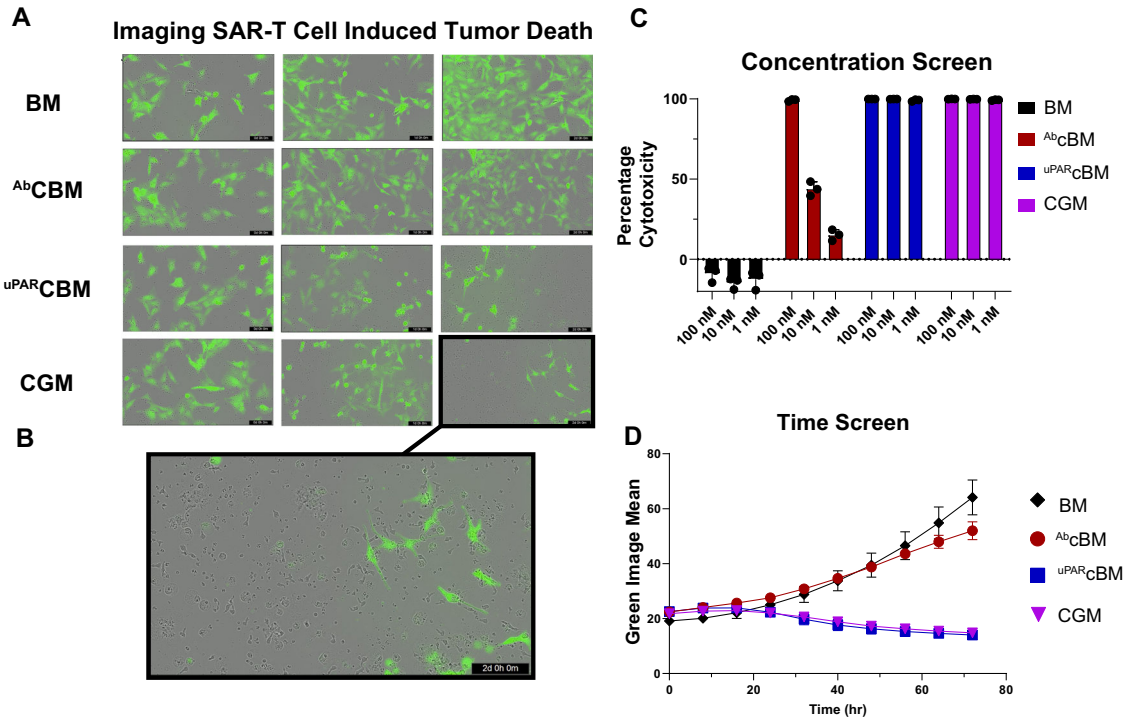

Fig. 5 | CGMs can induce cell-cell proximity activating tumoricidal T cell function. A Cytotoxicity assay using live cell microscopy monitoring A172 tumor cell death in SAR-T cell co-cultures as a function of time: Day 0 (left), Day 1, (middle), and Day 2, (right), uPAR+ A172s (green), SAR T-cells (grey). Top row: BM (100 nM). Second Row: ^{Ab}cBM (1 nM). Third Row: ^{uPAR}cBM (1 nM). Fourth Row: CGM (1 nM). **B** Day 2, 1 nM CGM condition, magnified, showing high density of SAR T cells illustrating T-cell proliferation and reduced tumor cell count. **C** Bar graph depiction of T-cell cytotoxicity quantification. **D** SAR T cell cytotoxicity time course, plotting Green Image Mean vs Time (h). Data was presented as mean +/− s.d. of $n = 3$ biologically independent samples.

covalently crosslinked ternary complexes is sufficient to enhance immunotherapeutic function via cell-cell induced proximity. This finding inspired us to investigate the potential origins of the observed sub-stoichiometric conversion in gel assays. Our studies in Fig. 2 support the efficient selectivity of each electrophile on CGM for the correct ternary complex protein. This means CGM conversion is unlikely limited by quenching of both electrophiles by either antibody or uPAR, or off target crosslinking. The SuFEx electrophiles used in CGM are also hydrolytically stable over the time-course of the above assays. These facts combined founded our hypothesis that CGM itself may degrade through alternative pathways to hydrolyze SuFEx. To test this, we pursued LC-MS time-course studies on free CGM in solution and discovered the formation of a cyclization product over the course of several hours (Supplementary Fig. S32, S33). We hypothesized this is facilitated by a proximal tyrosine on the CGM which can attack SuFEx. To test this hypothesis, we substituted the tyrosine on CGM with alanine to form CGM-AE137 and repeated LC-MS studies (Supplementary Fig. S32). These studies indicated complete abolishment of the cyclization product. Analysis of CGM-AE137 mediated ternary complex formation by SDS-PAGE also demonstrated a significant increase in conversion from ≈ 25% to 50% crosslinked ternary complex product by densitometry analysis (Supplementary Fig. S33).

Discussion

Herein we report a dual covalent chimera strategy to covalently crosslink ternary complexes with tumor immunotherapeutic function. We demonstrate incorporation of two strategic electrophiles within a synthetic chimeric molecule can be pre-organized to covalently crosslink two proteins efficiently and with high selectivity. This kinetically "mimics" molecular glues by stabilizing ternary complexes against dissociation events, that can be driven by depletion of binding partners, negative binding co-operativity, and/or the presence of competitive binding ligands.

Critical to accomplishing molecular glue mimicry using dual covalency, is the demonstrated ability of CGMs to efficiently discriminate between two bound ternary complex proteins. Achieving this high *intra* ternary selectivity by two electrophiles on the CBM while maintaining fast labeling kinetics, represents a unique developmental advance. CGM chimeras rely on reaction kinetic effective molarity to control the kinetics and selectivity of dual covalent crosslinking. This makes this strategy broadly applicable to crosslinking any two endogenous proteins where modest affinity binding ligands like peptides are available, and without dependence on cysteines. By tuning the electrophile pre-organization and reaction effective molarity, even modest affinity targeting ligands can be strategically leveraged. We observed SuFEx positioning dramatically modulates the rate of uPAR labeling, allowing for significant increases in labeling rate without needing to increase the intrinsic electrophile reactivity. This is advantageous since increasing the latter also favors hydrolysis and off-target labeling.

The comparable association signal observed for all covalent compounds in Fig. 3C indicate their comparable ability to form in-solution ternary complexes. If this holds true in the context of inducing proximity between tumor and immune cells, then the increased efficacy observed in our functional immune activation assays for CGM versus analogous chimeras, is related to the ability of covalently crosslinked ternary complexes to offset/overcome an intrinsic barrier to activating immune signaling. The decreased function associated with non-covalent BM despite its high (*nM*) solution binding affinities, suggests this barrier to activation signaling can destabilize cell associated ternary complexes that are thermodynamically favorable, when the same proteins are free in solution. This implies that in the context of cell-cell induced proximity, the efficacy of even high affinity chimeras may be limited by signaling barriers that impose mechanical and/or steric strain on ternary complexes[12,26]. Covalent crosslinking of the ternary complex would thus be expected to uniquely oppose these

destabilizing forces and overcome this barrier. The data in Fig. 3F, in the context of beads, suggests CGMs can now template more ternary complexes compared to analogous mono-covalent and non-covalent analogs, presumably by counteracting destabilizing interactions on the ternary complex induced by the proximity of the two surfaces. This is especially interesting given the likely avidity stabilization on non-covalent ternary complexes due to the multivalent display of uPAR and antibody on beads. The destabilizing forces directed on ternary complexes that bridge cells directly, may, therefore represent a broader challenge to proximity inducing molecules that lack glue function. These systems could uniquely benefit from our covalent chimera "glue mimic" strategy, which could present a complementary approach to bona fide molecular glue discovery or rational design.

CGM mediated conversion to covalently crosslinked ternary complex was estimated to be ≈ 25% in gel assays (Supplementary Fig. S20, S21) We identified a potential major factor limiting CGM conversion due to an interesting intramolecular cyclization reaction via tyrosine that quenches a reactive SuFEx. We also demonstrated by gel assays this can be easily circumvented via tyrosine substitution on the CGM to enhance conversion efficiency. Given the functional enhancements observed for CGM in cell assays, it appears quantitative conversion to covalently cross-linked ternary complexes is not necessary to enforce cell-cell proximity. This is likely especially true when directly crosslinking two cells using "irreversible" electrophiles. Future efforts in the lab aim to enhance conversion to covalently crosslinked ternary complexes in various therapeutic applications using reversible electrophiles, which are inert to hydrolysis and can correct for binding independent labeling. The lack of quantitative conversion observed for current CGMs could still be limited by electrophile hydrolysis induced from selective binding interactions itself, which is challenging to discern.

In the current work, antibody bridging (free or T cell associated) to the uPAR tumor antigen was chosen as an established ternary complex model system to develop CGMs, that leverages peptidic binding modalities. Peptides are gaining therapeutic momentum to drug cell surface receptors, are readily accessible with high receptor selectivity, and are associated with modest potency that can be efficiently enhanced through the facile incorporation of covalent binding electrophiles. The CGM approach is thus, highly applicable to other tumor antigens and immune receptors and indications beyond immunoncology that function through cell-cell induced proximity. In immuno-oncology applications of cell-cell induced proximity, we demonstrate CGMs can covalently crosslink ternary complexes, leading to increased tumoricidal immune function via both macrophage and NK cell receptor activation. We also demonstrate that the covalent engagement of the tumor antigen (not immune receptor) is critical for the activation of engineered universal T cells. The generality and mechanistic basis for this observation is currently being explored in our laboratory but is likely related to intrinsic differences in activation thresholds for native immune cells like macrophages, which is quite high, and engineered T cells, which is likely much lower. This lower activation threshold is consistent with the high tonic signaling associated with CAR-T cell therapies.

Despite the encouraging in vitro results above, there exist potential limitations to translation that require validation in future in vivo studies. Many of these limitations are already faced by current bi-specific antibody engager therapies that similarly bridge immune cells with tumor cells in a ternary complex. In contrast to bi-specific antibodies however, CGMs are chemically synthetic in nature, much smaller in size, and possess the unique ability to *covalently* engage their two target proteins. These properties combined may enhance the therapeutic efficacy of CGMs relative to bi-specific antibodies through increased in vivo stability and tumor penetration, in addition to increased stabilization of ternary complexes via covalency.

In vivo, CGM chimeras must covalently crosslink both ternary complex proteins quickly and selectively, before they are cleared from systemic circulation. Fast clearance from systemic circulation represents a limitation of current bi-specific antibodies and may similarly complicate the dosing of CGMs as therapeutics in vivo. Our in vitro data demonstrates conversion to the covalently crosslinked ternary complex occurs on the timescale of hours which is competitive with the projected clearance rates for low molecular weight modalities like CGMs. Although the kinetics of covalent ternary complex crosslinking are not fast enough for quantitative conversion prior to clearance, the clearance rate itself will be dramatically reduced after the first labeling event. This suggests that current CGMs can retain longer in vivo compared to current bi-specific antibodies, however, this requires pharmacokinetic validation in vivo.

A second potential limitation of the current iteration of CGMs in vivo is their selectivity for tumor and immune proteins. Off-target covalent labeling can induce undesirable toxicity that would not accompany treatment using bispecific antibodies that bind non-covalently. Analysis by SDS-PAGE, BLI and flow cytometry support CGMs are selective for target tumor and immune proteins versus abundant off-target serum proteins, supporting the likelihood they can engage intended targets efficiently in vivo. These assays, however, do not capture the complexity of off-target proteins that exist in an in vivo setting, including components of the metabolic machinery. Potential off-target labeling could be addressed using fast reacting reversible electrophiles that form kinetically favorable crosslinks like salicylaldehydes, but only when stabilized through proximal ligand binding.

Current CGMs are peptidic in composition, which could represent an enzymatic/metabolic liability in vivo similar to bi-specific antibodies, however, this can be addressed by efficiently substituting peptidic uPAR targeting ligands with available uPAR targeting small molecules, and available small molecule ligands for other tumor targets like prostate-specific membrane antigen (PSMA) and human epidermal growth factor receptor 2 (HER2).

In vivo, unique potential limitations to the current iteration of CGMs versus bi-specific antibodies is inhibition of catalytic turnover, preventing immune cells from recursive killing by covalently locking them with tumor cells. These potential limitations serve as additional rationale for our current efforts exploring the utility of reversible covalent electrophiles for cell-cell induced proximity and translation of the CGM strategy in vivo.

Methods

Ethics declaration

Engineering of human T cells research was approved by the McMaster Health Sciences Research Ethics Board (Approved IRB #15627 and #15643) and all donors in this study provided informed written consent. Peripheral blood mononuclear cells (PBMCs) were obtained from healthy donors (McMaster Adult Cohort (MAC) donor). In some cases, PBMC were collected from commercial leukapheresis products (HemaCare and StemCell Technologies) and isolated by Ficoll-Paque-Plus gradient centrifugation (GE Healthcare) and cryopreserved in inactivated human AB serum (Corning), containing 10% DMSO (Sigma-Aldrich), or Cryostor CS10 (StemCell Technologies).

Peptide synthesis and purification

All chemical reagents and solvents were obtained from commercial suppliers (Sigma Aldrich, ChemImpex) and used without further purification. All bifunctional molecules were synthesized using a Liberty Blue synthesizer. Deprotection was done using 0.1 M Oxyma, 20% Piperidine in DMF, for 1 minute at 90 degrees. Coupling was done using 1 M Oxyma and DIC, with 0.2 M Fmoc protected amino acids, in DMF, for 2 minutes at 90 degrees. The benzoic aryl sulfonyl fluoride was coupled at the *N* terminus on bead using standard Fmoc amide coupling chemistry. DNP was incorporated as a pre-synthesized Fmoc-Lys(DNP) building block (Chem Impex Cat. # 05734) and directly incorporated into the SPPS

workflow. When necessary, Fmoc-Lys-DDe was used to insert the uPAR labeling SuFEx electrophile. Lys-DDe was deprotected using 15 mL of 2% hydrazide for 15 minutes to orthogonally deprotect the DDe on bead. The benzoic aryl sulfonyl fluoride was then coupled using the free amine. Cleavage from the resin was accomplished using 95/2.5/2.5 TFA:H_2O:TiPS for 3 hours. Immediately after cleavage, HPLC and LCMS was conducted to purify and characterize the compound. LCMS data was obtained using an LTQ Orbitrap XL system with a gradient of 95:5 to 5:95 (Water, 0.1% formic acid: Acetonitrile, 0.1% formic acid). A ThermoFisher DIONEX UltiMate 3000 UHPLC+ was used for HPLC purification with a gradient of 90:10 to 10:90 (Water, 0.1% formic acid: Acetonitrile, 0.1% formic acid). This was then followed by lyophilization.

Biolayer Interferometry (BLI) assays on Octet

All Octet Assays were conducted using an Octet Red96e System (Sartorius). A volume of 200 µL of each solution was loaded onto a black flat-bottom 96-well plate (Grenier). Probes were always pre-wet for 10 minutes in 1X Kinetics Buffer (Sartorius) prior to the experiment. For ^{uPAR}cGM kinetics, 300 nM of ^{uPAR}cGM was incubated with 75 nM uPAR-Biotin from Acro Biosystems (Cat. No. UPR-H82E7) for various amounts of time. At the end of the incubation time a final concentration of 10 µM of AE105 uPAR competitor was used to quench the reaction. Streptavidin probes were placed in 1X Kinetics Buffer for 2 minutes to establish a baseline. This was followed by placing the probes in the timed incubation solution above, for 3 minutes. The probes were placed in 1X Kinetics Buffer for 3 minutes in order to re-establish a baseline. Next, they were added to a 250 nM Anti-DNP solution in 1X Kinetics Buffer for 5 minutes to measure the association. For ^{Ab}cBM kinetics, 300 nM of ^{Ab}cBM was incubated with 75 nM of Anti-DNP Ab for various amounts of time. 200 µM of DNP-Glycine competitor was used to quench the reaction. ProG probes (Sartorius) were placed in 1X Kinetics Buffer for 2 minutes to establish a baseline. This was followed by submerging the probes in the timed incubation solution above, for 3 minutes. The probes were then placed in 1X Kinetics Buffer for 3 minutes to re-establish a baseline. Next, they were added to the 500 nM uPAR solution in 1X Kinetics Buffer for 5 minutes to measure the association. For ^{uPAR}cBM derivative kinetics, the above experiment was repeated, except the incubation time was 2 hours. For ^{Ab}cBM terminal protein selectivity, 250 nM ^{Ab}cBM was incubated with 100 nM uPAR-biotin overnight. Streptavidin probes were placed in 1X Kinetics Buffer for 2 minutes to establish a baseline. This was followed by placing the probes in the incubated solution above, for 3 minutes. The probes were placed in 1X Kinetics Buffer for 3 minutes in order to re-establish a baseline. Next, they were added to a 250 nM anti-DNP solution to measure association.

For ^{Ab}cBM terminal protein selectivity, ^{uPAR}cBM and ^{uPAR}CBM-2 was incubated with 250 nM Ab overnight. The next day 200 µM DNP-glycine competitor was added to quench the reaction and disrupt any non-covalent complex. Streptavidin probes were placed in 200 µL of 1X Kinetics Buffer, to pre-wet for ten minutes. Next, the probes were placed in 1X Kinetics Buffer for 2 minutes to establish a baseline. This was followed by submerging the probes in a 100 nM solution of uPAR-Biotin from Acro Biosystems for 3 minutes. The probes were then placed in 1X Kinetics Buffer for 3 minutes in order to re-establish a baseline. Next, they were added to the 500 nM bifunctional molecule + 250 nM Anti-DNP + 200 µM DNP-Glycine solution in 1X Kinetics Buffer for 5 minutes to measure the association. For dual covalent reaction labeling, 100 nM bifunctional molecule was incubated with 100 nM uPAR biotin + 50 nM Anti-DNP overnight. The next day Streptavidin probes were placed in 1X Kinetics Buffer for 120 seconds to establish a baseline. This was followed by placing the probes in the incubated solutions above, for 3 minutes. The probes were then placed in 1X Kinetics Buffer with 10 µM AE105 competitor for 4 minutes. Next, they were added to a 50 µM DNP competitor solution for 5 minutes.

SDS-PAGE

For each gel, 4 to 20%, Tris-Glycine, 1.0 mm, Mini Protein Gels from Invitrogen (Catalog # XP04202BOX) were used. 2 µM uPAR was mixed with 0.6 µM Anti-DNP Ab, with 2.5 µM bifunctional molecule overnight. All samples were mixed with BioRad 4x Laemmli sample buffer (Catalog #161-0747) and heated at 95 °C for 2 minutes prior to loading on the gel. All gels were run in an Invitrogen mini gel tank at 90 V for the length of the stacking gel and 120 V for the length of the resolving gel. Once stained with EZ-Blue Gel Staining solution (Sigma), the protein contents were visualized using a 700 nM laser on an Odyssey CLX imager. For the Densitometry analysis ImageJ software was used.

AlphaLISA experiment for covalent ternary complex crosslinking

AlphaLISA immunoassay Buffer (10X) (Revvity, Cat. # AL00C) was diluted 10X with Milli Q water and used for all dilutions. A solution of 300 nM uPAR-Biotin, 300 nM Anti-DNP Ab, and 300 nM of Chimera was preparred. Following an overnight incubation, post-comp solutions were incubated with AE105 competitor + DNP competitor (to a final concentration of 2.5 µM and 12.5 µM, respectively) and left for 15 minutes. A 1:100 dilution of 5 mg/mL AlphaLISA anti-human IgG acceptor beads (Revvity, Cat. # AL103C) and 5 mg/mL AlphaLISA streptavidin donor beads (Revvity, Cat. # 6760002S), was prepared and 8 µL were placed in a AlphaPlate light grey 384 well plate (Revvity, 60005350). Next, 1 µL of the Chimera + protein solution incubations were diluted to a final concentration of 5 nM. 12 µL of the Chimera + protein solution incubations (5 nM) were mixed in the plate and left to incubate at r.t. for 1 hour. The plate was covered by aluminum foil to prevent exposure to light. A TECAN Spark plate reader was used on the AlphaLISA Technology setting to assess counts/second.

Cell surface covalent ternary complex crosslinking

A 20:1 molar ratio of BroadPharm Fluor 647 NHS Ester (Catalog # BP-24069) was mixed with 12.25uM Anti-DNP Ab at room temperature for 1 hour. NAb Protein A Plus Spin Columns, 0.2 mL (Thermo Scientific) were used to remove free dye. A final concentration of 1.23 mg/mL of SPE7-AF647 was calculated using a NanoDrop UV-Vis Spectrophotometer (Thermo Scientific). uPAR+/− A172 cells were suspended using 1 mM EDTA and quenched with complete growth media. The cells were seeded at a concentration of 1,500,000 cells/mL using serum free assay media (neat DMEM). To a U-bottom 96-well plate (Fischer Scientific V22887), 100 µL of cells were added to 1 µM of CGM or BM and 500 nM SPE7-AF647 and placed in a 37 °C 5% CO_2 incubator for 4 hours. All samples were washed three times with serum free assay media (neat DMEM), and plates were placed on ice before running flow cytometry. The following gains were used, FSC: 81 SSC: 109 APC: 200

Cell culture

All flow cytometry experiments were run on a Beckman Coulter CytoFLEX Flow Cytometer or a BD LSR II. The human IgG isotype control used was purchased from Jackson ImmunoResearch (Cat. No. 009-000-003). For uPAR selectivity controls, AE133 competitor peptide lacking the DNP moiety was used. A172 cells were purchased from ATCC (Cat. No. CRL-1620). U937 cells were generously given by Dr. John Valliant (McMaster University, Canada). IFN-γ was purchased from Fischer Scientific (PHC4031). Ultra-low IgG FBS was purchased from Fischer Scientific (A3381901). DiD cell dye was purchased from Fischer Scientific (V22887). 96-Well U-bottom plates were purchased from Fischer Scientific (08-772-17). Pen/Strep was purchased from Fischer Scientific (15140-122). FBS was purchased from Fischer Scientific (12484-028).

uPA-uPAR competition experiment via widefield microscopy

A 20:1 molar ratio of BroadPharm Fluor 647 NHS Ester (Catalog # BP-24069) was mixed with 25 µM Human uPa Protein (Acro Biosystems,

PLU-H5229) at room temperature for 1 hour. To purify the protein conjugates, NAb Protein A Plus Spin Columns, 0.2 mL (Thermo Scientific) were used. A final concentration of 20.75 uM of uPa-AF647 was calculated using a NanoDrop UV-Vis Spectrophotometer (Thermo Scientific). uPAR+ A172 cells were lifted using 0.5% Trypsin-EDTA (Gibco) and quenched with complete growth media. 100 μL of cells were seeded at a concentration 50,000 cells/mL. 50 μL of 100 nM CGM or BM were added to cells for 15 minutes prior to washing the cells and adding 100 μL of 25 nM of uPa-AF647. Samples were washed again and imaged on a Zeiss Celldiscoverer7 inverted widefield microscope, using a Plan-Apochromat 20x/0.7 NA lens with a Colibri light source. uPa-AF647 was detected using a 631/33 nm excitation filter and a 687/145 nm emission filter. The nuclei were stained using DAPI, detected using a 385/30 nm excitation wavelength, and a 425/30 nm emission filter. The DAPI and the AF647 Channel were at 10.00% and 27.50% LED power, respectively. The sample was acquired with an Axiocam 712 mono camera, exposure time was set to 55 ms and 175 ms for the DAPI and AF647 channel, respectively. Images were acquired using ZenBlue software.

Antibody dependent cell mediated phagocytosis (ADCP) assay

For preparation of effector monocytes, 24 hours prior to inducing phagocytosis, U937 monocytes were seeded at 5×10^5 cells/mL and activated with IFN-γ (0.1 mg/mL). After incubation, cells were counted and washed twice with serum free assay media (neat DMEM). Cells were then suspended to a concentration of 1 million cells/mL and stained with 1.9 μM Vybrant DiD Cell-Labeling Solution for 30 minutes (37 °C, 5% CO_2). Cells were then washed 3x with warm assay media (AM, 14% Ultra Low IgG FBS in DMEM) and resuspended to a concentration of 3.0×10^6 million cells. The day prior, 100 nM Biotin-uPAR + 200 nM bifunctional molecule + 100 nM anti-DNP Ab was incubated overnight. The next day 10 million Streptavidin YG beads (Polysciences Cat. #24157) were washed 2X with PBS. The uPAR biotin, anti-DNP Ab, and bifunctional molecule solution was then incubated with 1.5×10^5 Streptavidin beads for 1 hour. Next, the beads were washed and combined with 1.5×10^5 monocytes. Next, the solutions were spun down at 800 RPM and incubated at 37 degrees for 1 hour. This was followed by placing solutions on ice to end phagocytosis, prior to flow cytometry analysis. Quadrant 1 represents target bead population only. Quadrant 2 represents the engulfed target bead population. ADCP percentage was calculated by dividing Q2/(Q2 + Q1) X 100%. The following voltages were used FSC: 330 SSC: 270 PE: 310: AF647: 400.

CD16α activation assay

ADCC was quantified using the ADCC Reporter Bioassay kit (Promega G7010). Target cells were seeded at a density of 2.5×10^4 cells per well in opaque 96 well flat-bottom plates (Corning Costar, 3917) in complete media. Sixteen hours after seeding, cells were washed gently with 100 μL of neat RPMI. To the cells, 25 μL of RPMI supplemented with 4% ultra-low IgG FBS was added, followed by 25 μL of a dilution series starting at 250 nM of BM, ^{Ab}cBM, ^{uPAR}cBM, or CGM with 125 nM antibody. After a 45-minute incubation, 2 μL of supplemented RPMI containing 7.5×10^4 Jurkat effector cells expressing human CD16 were added to each well. The plates were then incubated for 24 additional hours. 75 μL of Bio-Glo Luciferase Assay Reagent was added to each well, and luminescence was quantified using the SpectraMax i3 plate reader.

Receptor generation and gamma retrovirus production for SAR-T cell system

The SPE7 variable heavy-variable light (VHVL) scFv was first designed using the crystal structure (PDB: 1OAU) and synthesized by Genscript. Human CD8α signal peptide was used. The anti-DNP scFv containing engineered receptors were cloned into the pRV100G backbone. Gammaretrovirus was generated to be used for subsequent engineering of T cells. Briefly, PLAT-E cells were first transduced with the anti-DNP SAR containing plasmids (15 ug) and pCl Eco (15 μg) using Opti-MEM (Gibco) and Lipofectamine 2000 (Thermo Fisher Scientific). Ecotropic gamma retrovirus was concentrated by centrifugation in Amicon filter system (Millipore Sigma) and stored at −80 °C. This virus was then used to transduce PG-13 cells. After 3 days of consecutive transduction, the PG13's were scaled up and subsequently the virus containing supernatant was filtered through a 0.45 μm filter (Brand) and stored at −80 °C to be used for T cell engineering.

Engineering of human T cells

To produce primary human *αβ* T cells, $1X10^6$ PBMCs were seeded in a 24 well plate and stimulated with ImunnoCult CD3/CD28/CD2 soluble activator (Stemcell) at a concentration of 25 μL/mL and cultured in RPMI 1640 containing 10% FBS, 10 mM HEPES (Roche Diagnostics), 1 mM sodium pyruvate (Sigma-Aldrich), 1 mM non-essential amino acids (Gibco), 55 μM β-mercaptoethanol (Gibco), 100 U/mL penicillin (Gibco), 100 μg/mL streptomycin (Gibco), 100 I.U./mL rhL-2 and 10 ng/mL rhIL-7 (PeproTech). 48 hours later, cells were transferred to a 24 well non tissue culture coated plate (Falcon) that was pre coated with retronectin (10 ug/mL) and anti-DNP scFv SAR gamma retrovirus for transduction. 24 hours later 1 mL of T cell media supplemented with rhL -2 (100 I.U./mL,1.5 ng/ml) and rhIL-7 (10 ng/mL) (PeproTech) is added to each well. 48 hours after the media addition the cells are washed with PBS and scaled into a larger vessel. Cells were cultured for a total period of 14 days prior to cryopreservation. T cells were cryopreserved in Cryostor CS10 (StemCell Technologies) according to manufacturer's instructions.

Live cell killing assay with SAR-T cell system

A172 glioblastoma cells were engineered with eGFP lentivirus made in house. In these experiments 5×10^3 tumor cells per well were plated in a 96 well flatbottom plate overnight. The next day anti-DNP SAR αβ T cells were added to the tumor cells at an effector to target ratio of 8:1. Also added to the wells were the bifunctionals at various concentrations (1 nM, 10 nM, 100 nM). The 3 components were co-cultured for 3 days at 37 °C and 5% CO_2 in the Sartorius Incucyte S3 Live cell imaging system with 9 images per well taken every 8 hours. For the A172 eGFP cells, the green image mean for each image was used to determine tumor cell growth. The area under the growth curve (AUC) was analyzed using Prism GraphPad and used as a metric for tumor cell growth for this data. The larger the area, the greater the tumor cell growth that occurred over the incubation period. The area under the curve for the tumor alone control and each condition were used to calculate the % cytotoxicity. Percent cytotoxicity was calculated as: (AUC Tumor Alone − AUC Sample)/(AUC Tumor Alone) X 100%.

Reporting summary

Further information on research design is available in the Nature Portfolio Reporting Summary linked to this article.

Data availability

Source data are provided with this paper as a Source Data file. Source data are provided with this paper.

References

1. Stanton, B. Z., Chory, E. J. & Crabtree, G. R. Chemically induced proximity in biology and medicine. *Science* **359**, eaao5902 (2018).
2. Gerry, C. J. & Schreiber, S. L. Unifying principles of bifunctional, proximity-inducing small molecules. *Nat. Chem. Biol.* **16**, 369–378 (2020).
3. Banaszynski, L. A., Liu, C. W. & Wandless, T. J. Characterization of the FKBP.rapamycin.FRB ternary complex. *J. Am. Chem. Soc.* **127**, 4715–4721 (2005).

4. Michnick, S. W., Rosen, M. K., Wandless, T. J., Karplus, M. & Schreiber, S. L. Solution structure of FKBP, a rotamase enzyme and receptor for FK506 and rapamycin. *Science* **252**, 836–839 (1991).
5. Schreiber, S. L. The Rise of Molecular Glues. *Cell* **184**, 3–9 (2021).
6. Douglass, E. F. Jr., Miller, C. J., Sparer, G., Shapiro, H. & Spiegel, D. A. A comprehensive mathematical model for three-body binding equilibria. *J. Am. Chem. Soc.* **135**, 6092–6099 (2013).
7. Murelli, R. P., Zhang, A. X., Michel, J., Jorgensen, W. L. & Spiegel, D. A. Chemical control over immune recognition: a class of antibody-recruiting small molecules that target prostate cancer. *J. Am. Chem. Soc.* **131**, 17090–17092 (2009).
8. Lake, B., Serniuck, N., Kapcan, E., Wang, A. & Rullo, A. F. Covalent immune recruiters: tools to gain chemical control over immune recognition. *ACS Chem. Biol.* **15**, 1089–1095 (2020).
9. McCann, H. M. et al. Covalent immune proximity-induction strategy using SuFEx-engineered bifunctional viral peptides. *ACS Chem. Biol.* **17**, 1269–1281 (2022).
10. Lake, B. P. M. & Rullo, A. F. Offsetting low-affinity carbohydrate binding with covalency to engage sugar-specific proteins for tumor-immune proximity induction. *ACS Cent. Sci.* **9**, 2064–2075 (2023).
11. Rakshit, S., Zhang, Y., Manibog, K., Shafraz, O. & Sivasankar, S. Ideal, catch, and slip bonds in cadherin adhesion. *Proc. Natl Acad. Sci. USA* **109**, 18815–18820 (2012).
12. Jeffreys, N., Brockman, J. M., Zhai, Y., Ingber, D. E. & Mooney, D. J. Mechanical forces amplify TCR mechanotransduction in T cell activation and function. *Appl Phys. Rev.* **11**, 011304 (2024).
13. Kapcan, E. & Rullo, A. F. A covalent opsonization approach to enhance synthetic immunity against viral escape variants. *Cell Rep. Phys. Sci.* **4**, 101258 (2023).
14. Dong, J., Krasnova, L., Finn, M. G. & Sharpless, K. B. Sulfur(VI) fluoride exchange (SuFEx): another good reaction for click chemistry. *Angew. Chem. Int Ed. Engl.* **53**, 9430–9448 (2014).
15. Zheng, Q. et al. SuFEx-enabled, agnostic discovery of covalent inhibitors of human neutrophil elastase. *Proc. Natl Acad. Sci. USA* **116**, 18808–18814 (2019).
16. Mortenson, D. E. et al. Inverse drug discovery" strategy to identify proteins that are targeted by latent electrophiles as exemplified by aryl fluorosulfates. *J. Am. Chem. Soc.* **140**, 200–210 (2018).
17. Somsen, B. A. et al. Reversible dual-covalent molecular locking of the 14-3-3/ERRgamma protein-protein interaction as a molecular glue drug discovery approach. *J. Am. Chem. Soc.* **145**, 6741–6752 (2023).
18. Zhai, B. T. et al. Urokinase-type plasminogen activator receptor (uPAR) as a therapeutic target in cancer. *J. Transl. Med.* **20**, 135 (2022).
19. Ploug, M. et al. Peptide-derived antagonists of the urokinase receptor. affinity maturation by combinatorial chemistry, identification of functional epitopes, and inhibitory effect on cancer cell intravasation. *Biochemistry* **40**, 12157–12168 (2001).
20. Llinas, P. et al. Crystal structure of the human urokinase plasminogen activator receptor bound to an antagonist peptide. *EMBO J.* **24**, 1655–1663 (2005).
21. Lallemand, C. et al. A novel system for the quantification of the ADCC activity of therapeutic antibodies. *J. Immunol. Res* **2017**, 3908289 (2017).
22. Kapcan, E., Lake, B., Yang, Z., Zhang, A., Miller, M. S. & Rullo, A. F. Covalent stabilization of antibody recruitment enhances immune recognition of cancer targets. *Cell Chem. Biol. Rev.* **60**, 1447–1458 (2021).
23. Jenkins, M. R., Tsun, A., Stinchcombe, J. C. & Griffiths, G. M. The strength of T cell receptor signal controls the polarization of cytotoxic machinery to the immunological synapse. *Immunity* **31**, 621–631 (2009).
24. Serniuck, N. J. et al. Electrophilic proximity-inducing synthetic adapters enhance universal T cell function by covalently enforcing immune receptor signaling. *Mol. Ther. Oncol.* **32**, 200842 (2024).
25. Kim, M. S. et al. Redirection of genetically engineered CAR-T cells using bifunctional small molecules. *J. Am. Chem. Soc.* **137**, 2832–2835 (2015).
26. Huse, M. Mechanical forces in the immune system. *Nat. Rev. Immunol.* **17**, 679–690 (2017).

Acknowledgements

We wish to thank our funding sources, the NSERC Discovery Grant program and the Canadian Cancer Research Society Operating Grant program #941832.

Author contributions

Synthesis, BLI, and Flow Cytometry was completed by E.K., K.K. ran alphaLISA assays, CGM stability assays and SDS-PAGE assays and contributed to manuscript preparation. M.D.L. performed SDS-PAGE, microscopy competition experiments and Ab Recruitment. N.J.S. and J.B. helped conceive and perform SAR-T molecular and cellular work. A.Z. performed CD16 activation assay. J.B. is co-supervisor of N.J.S. E.K., and A.F.R. conceived of project, interpreted experimental results and wrote the manuscript.

Competing interests

E.K., K.K., M.D.L., and A.F.R. are co-inventors on a patent related to CGMs. N.S., E.K., A.F.R., J.L.B. are co-inventors on a patent related to universal SAR-T cells. The remaining authors declare no competing interests.

Additional information

Supplementary information The online version contains supplementary material available at https://doi.org/10.1038/s41467-025-58083-z.

Correspondence and requests for materials should be addressed to Anthony F. Rullo.

Peer review information *Nature Communications* thanks M. Cristina Vega, Hua Wang and the other anonymous reviewer(s) for their contribution to the peer review of this work. A peer review file is available.